Final Report, Grant NCC3-968
6/1/02 – 10/6/03

NASA John H. Glenn Research Center
Michael A Meador, PhD, Chief, Polymer Branch

Submitted by

The University of Akron
Darrell H. Reneker, Professor of Polymer Science
dhr@polymer.uakron.edu
University Circle, Akron, OH 44325-3909
330-972-6949

May, 2005

Polymer based nanocomposites with nanofibers and exfoliated clay

Objective

Produce polymer based composites, using nanofiber based approaches, in the form of strong, impermeable thin films and sheets. Characterize the morphology of exfoliated clay in sheets and nanofibers, using electron microscopy and electron diffraction.

Approach proposed

Polymer nanofibers will be electrospun from dispersions of exfoliated clay in solutions of polymers. Morphology of clay layers inside nanofibers will be observed using electron microscopy.

Nanofibers containing exfoliated clay will provide excellent samples for observation without the necessity for preparing microtomed thin sections if the nanofibers are thin enough.

For relatively big electrospun fibers, plasma etching will be used to thin the sample for transmission electron microscopy observation.

Electrospun nanofibers will be used to produce useful orientation of clay layers, which will reduce gas permeability.

What has been done?

1. Preparation and observation of electrospun fibers from polymer and exfoliated clay

Electrospun polymer fibers with and without clay were prepared by electrospinning from dispersions of exfoliated clay sheets in polymer solutions. Ribbon shaped polyimide fibers, with and without clay sheets, were observed by scanning electron microscopy. Clay sheets were completely embedded in fibers because the size of fiber was larger than the lateral size of clay sheets.

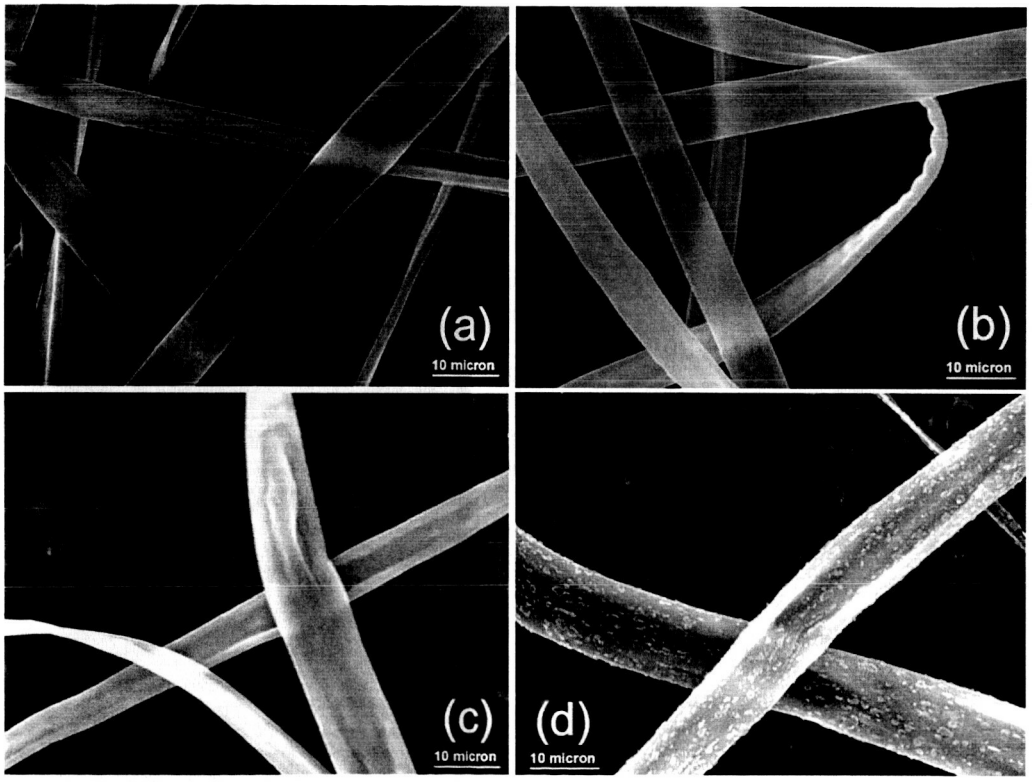

Figure 1. Scanning electron micrographs of pure polyimide fiber before (a) and after (b) plasma etching. Electrospun polyimide with clay sheets before (c) and after (d) plasma etching.

Plasma etching chamber was built in our laboratory with controlled etching rate. Active oxygen species were produced from a glow discharge. Polymers were removed from the surface of electrospun fibers and clay sheets buried underneath were exposed. Scanning electron micrographs of pure polyimide fibers and polyimide fibers containing clay sheets were obtained

on samples after etching. For pure polyimide fibers, no obvious morphological change was observed on as-spun fibers (Figure 1a) and fibers after etching (Figure 1b).

Similar ribbon shaped fibers with rather smooth surface were observed in as-spun polyimide fiber with clay (Figure 1c). Flake shaped particles were observed on the surface of electrospun fibers from polyimide and clay after removal of polymer by plasma etching (Figure 1d). These flakes on the surface of etched fibers were clay sheets that were buried inside fibers.

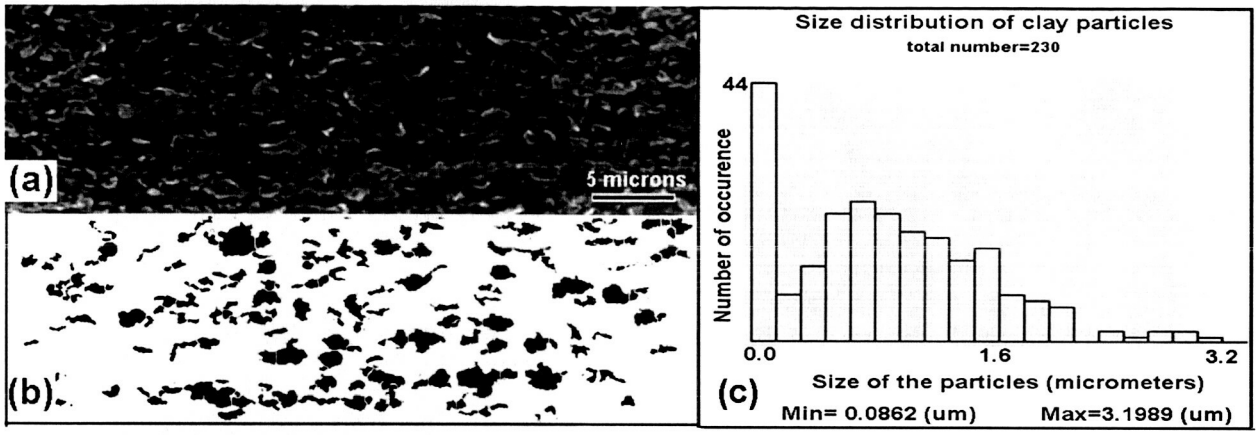

Figure 2. Size distribution of clay sheets revealed by plasma etching. (a) Original scanning electron micrograph of a segment of fiber surface after plasma etching; (b) Image processed to show individual particles; (c) Size distribution of all exposed clay sheets.

Quantitative analysis was carried on an area (Figure 2a) cut from the larger fiber after plasma etching. The dimensions of clay particles were measured in a higher magnification image. The software used to analyze the image was Photoshop® with a plug-in of Fovea Pro®. First, to separate individual clay sheets, threshold was applied to the image followed by watershed (Figure 2b). Second, the size of an individual sheet was characterized by the maximum distance between any two points that were both on the same sheet. The size can be automatically measured and labeled on the image. Finally, size distribution of the sample was plotted in Figure 2c. The size of clay sheets with largest population ranged from 600nm to 800nm across. There were also many smaller sheets in the image. This technique can be extended to other composite systems with fillers in various shapes.

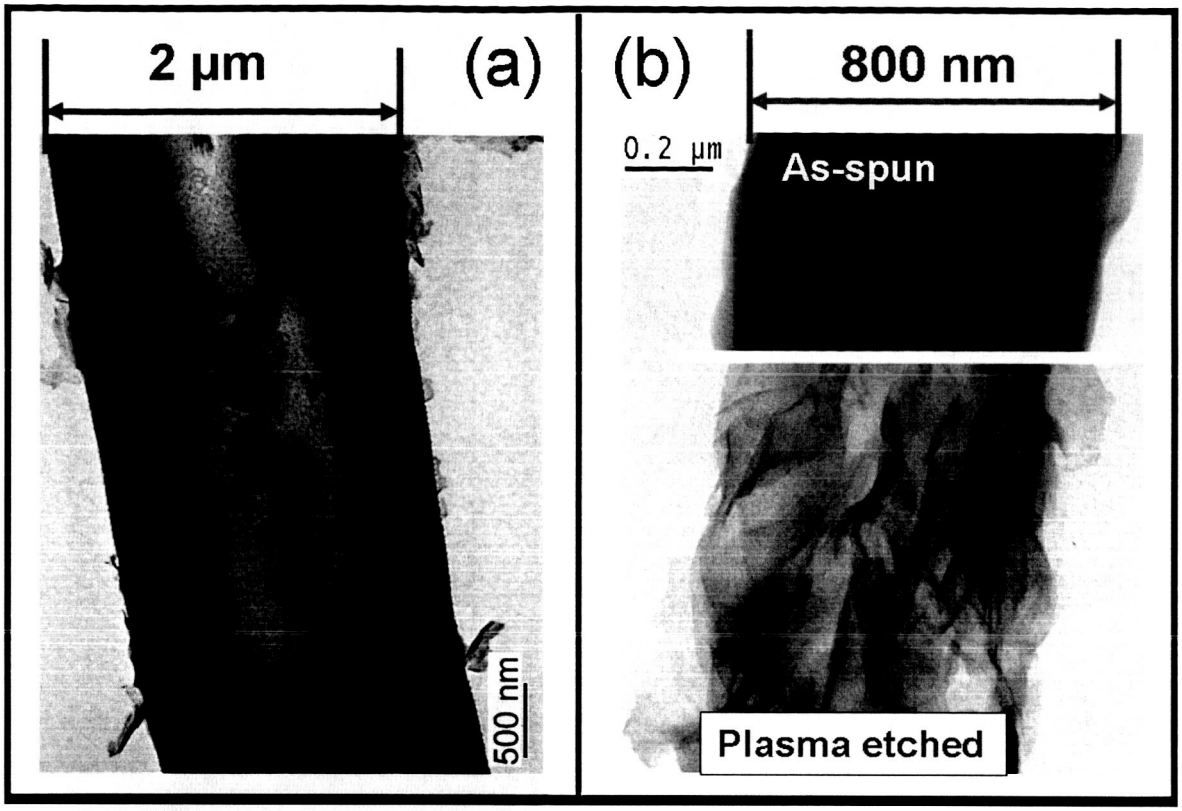

Figure 3. Arrangement of clay sheets inside electrospun fibers. (a) A 2 micrometers fiber; (b) A 800 nm fiber before (upper) and after (lower) plasma etching.

With fiber size larger than lateral size of clay sheets, the clay sheets tended to randomly orientated inside fiber as in bulk materials. Figure 3a shows a ribbon shaped polyimide fiber containing clay sheets with a width of two micrometers. The clay sheets were only partially aligned in the fibers. The direction normal to montmorillonite sheets tended to be perpendicular to the fiber axis due to jet flow and stretching process during the formation of fiber. The edges of the fiber were darker than the middle part in transmission electron microscope because of the dog-bone shape of a cross section of the ribbon. Clay sheets with irregular shape were observed as dark sheets lying in the middle part of the fiber if viewed along their normal direction. The dark curved lines were clay sheets viewed from edge. Some clay sheets were sticking on the surface after the removal of the surrounding polymer.

The arrangement of clay sheets was observed in a fiber with a diameter of 800 nm, which is comparable to the lateral size of clay sheets. The nanocomposite of polystyrene and montmorillonite was prepared by in-situ free radical polymerization of styrene monomer on the

surface of clay sheets. Polystyrene fibers containing clay sheets were electrospun from the resulting dispersion of the clay in a solution of polystyrene in THF. Figure 3b (upper) shows an electron micrograph of a segment of a polystyrene nanofiber that contained exfoliated montmorillonite sheets. The as-spun fiber was not transparent in the electron microscope due to the thickness of the fiber. A segment of a similar nanofiber showed clay sheets crumpling in the fiber after it was thinned by plasma etching (Figure 3b lower). The crumpling was resulted from the effects of the surface tension and elongational flow on the clay sheets during electrospinning. The clay particles are less crumpled in the axial than in the radial direction, indicating that the clay sheets can be expected to provide improvements in the tensile properties of the nanofiber. The crumpling of clay sheets inside a fiber, or inside a constraint environment, demonstrated the flexibility of clay sheets.

2. Observation of single clay sheets

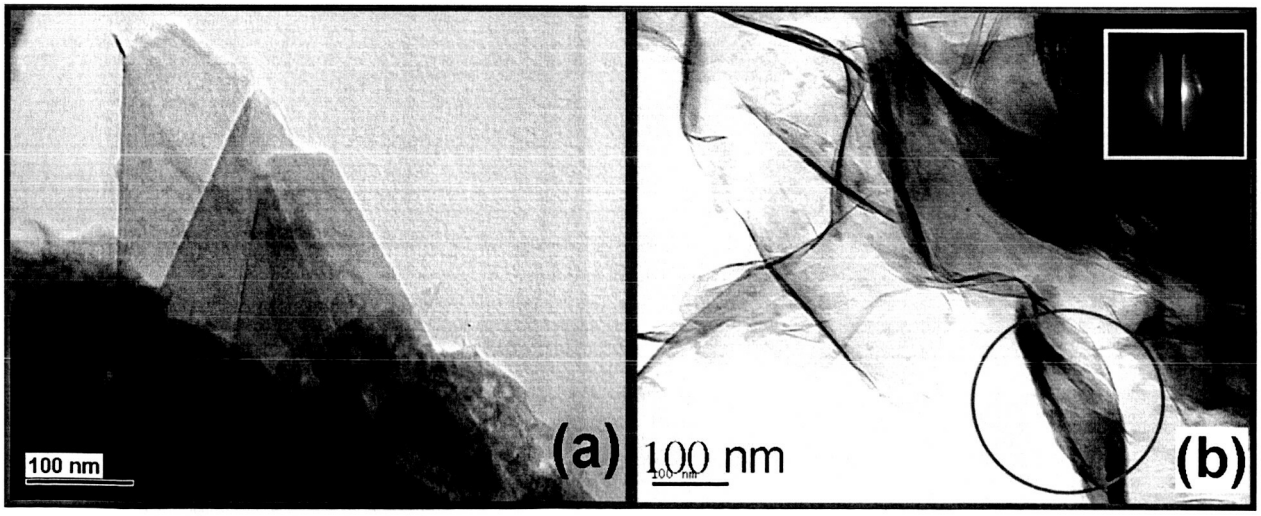

Figure 4. Observation of single clay sheets. (a) Clay sheets caught on electrospun fiber by filtering a suspension of clay in water through fiber mat; (b) Clay sheets exposed by plasma etching on a fiber with clay sheets inside.

Single clay sheets have irregular shape with a thickness of 1 nm and a lateral size of a few hundred nm. Observation of single clay sheets were carried out in two ways. First, clay particles were dispersed in water and sonicated for a few hours. A droplet of suspension was filtered through an electrospun fiber mat. Stacks of clay sheets were physically attached to the surface of

a fiber (Figure 4c). Second, a thin layer of polymer was removed from the fiber by plasma etching at a slow rate. By zooming-in to the surface of a fiber, clay sheets were observed to be flexible and easy to fold. The darker black lines in Figure 4b came from folded edges of clay sheets, or stacks of clay sheets. Some of the polymer, which was protected from the plasma by the sheets, held the sheets together after etching. Electron diffraction pattern (Inset in Figure 4b) was obtained from a selected area indicated by a red circle. The orientation of the stack of clay sheets resulted in the arch pattern.

3. Gas barrier film made from clay and electrospun fibers

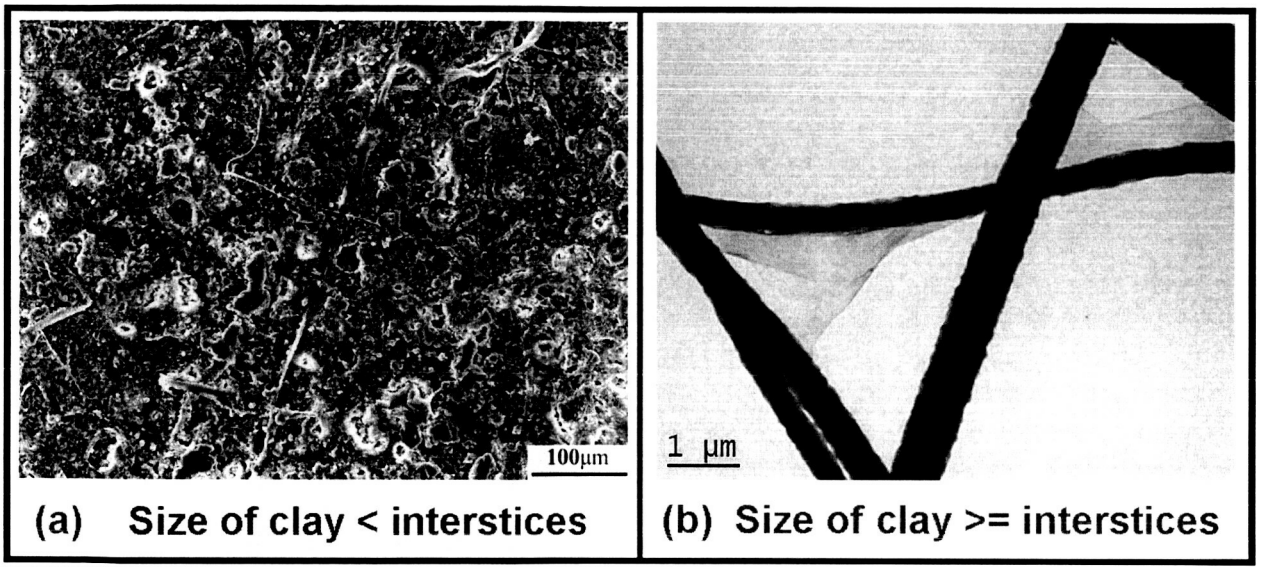

Figure 5. Arrangement of clay particles on fibers. (a) Montmorillonite particles supported on electrospun fibers; (b) Li^+-fluorohectorite supported on electrospun fibers.

Clay minerals, with layered structure, demonstrated improvements in the gas barrier properties at low concentration due to their high aspect ratio. The introduction of fillers resulted in a longer diffusive path for gas molecules and hence reduced permeability of the composite film. Due to its high aspect ratio, layered structure is particular efficient at maximizing the gas path compared to fillers in shapes of spheres or rods.

Lower relative permeability could be achieved by the following ways: (1) clay sheets with larger lateral size, (2) higher degree of exfoliation, (3) higher concentration of clay in polymer matrix, and (4) orientation perpendicular to gas diffusion direction. This work focused on lateral

size of clay sheets and orientation of clay sheets. Three types of clay, used in the laboratory, were Laponite® (lateral size of about 25 nm), organic modified montmorillonite (600 nm to over one micrometer) and Li^+-fluorohectorite (a few micrometers across). Electrospun nanofibers were used as filters or reinforcing scaffold for the gas barrier film.

When clay sheets are smaller than interstices between fibers, clay sheets tended to accumulated on the fiber mat and no obvious orientation of clay sheets was observed. Top view of the composite film from polymer nanofibers and particles of montmorillonite showed a rough surface (Figure 5c). Clay particles were physically attached to the fiber mat and no binder was used to fill the holes between clay particles. Poor gas barrier property was expected from the composite film according to morphology of the film.

When clay sheets are comparable or larger than interstices, clay sheets tend to lie flat on a fiber mat. Polyacrylonitrile fibers with diameters of a few hundred nanometers were electrospun from a solution of polyacrylonitrile in DMAc. Li^+-fluorohectorite suspended in water was filtered through the mat of electrospun fibers. Figure 5b showed a few sheets of Li^+fluorohectorite supported over an opening in a network of nanofibers. The exfoliated clay sheets tended to flat on and fill the interstices.

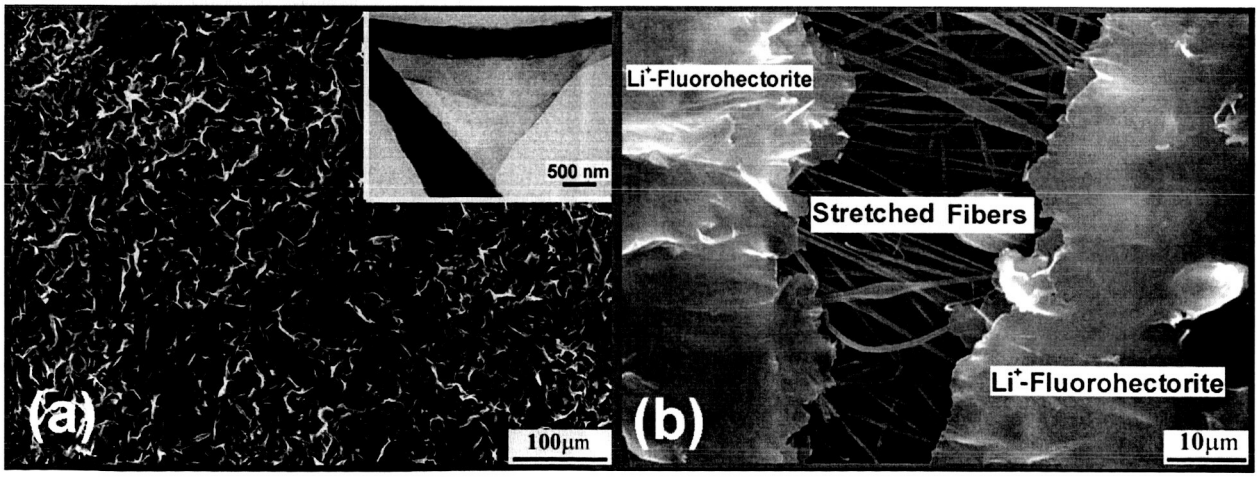

Figure 6. Continuous film of Li+-fluorohectorite supported on electrospun fibers. (a) Top view; (b) Tearing edge of the film.

By increasing the amount of Li^+-fluorohectorite in the filtration process, interstices between fibers were filled by the clay sheets. Macro scale gas barrier film was prepared from Li^+-

fluorohectorite and electrospun fibers. Accumulation of Li^+-fluorohectorite resulted in a continuous film of Li^+-fluorohectorite supported on electrospun fiber mat. The top surface of the constructed film was shown in (Figure 6a). It contained no holes visible in electron micrographs. Folding was widely observed on the surface of the film, which indicated the flexibility of Li^+-fluorohectorite. Figure 6b showed a scanning electron micrograph of a deliberately torn part of the film that exposed both the edges of the clay sheets and the fibers on which the layer of clay sheets was supported. There may be small channels along the edges of the individual clay layers. We expected that adding a polymer, which solidifies in the channels, to the mixture from which the Li^+-fluorohectorite sheets were collected, could block such channels. The electrospun fiber mats not only supplied the mechanical strength as a substrate but also introduced orientation of Li^+-fluorohectorite sheets so that clay sheets were lying flat inside film

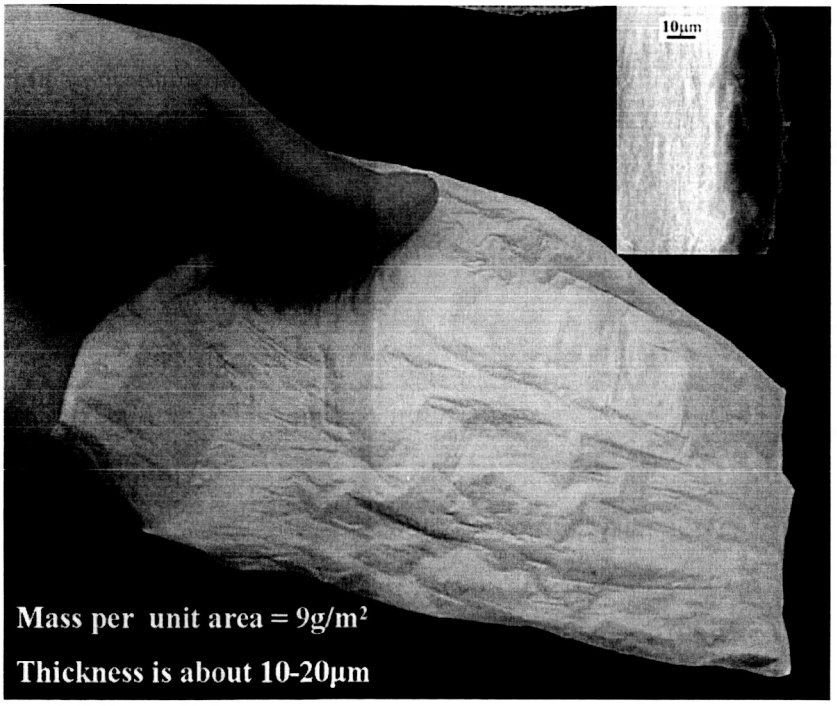

Figure 7. Larger piece of membrane with of Li+-fluorohectorite supported on electrospun fibers. Inset shows the thickness of the membrane.

Similar composite film was obtained by simply brushing the suspension of Li^+-fluorohectorite on electrospun fiber mats so that larger pieces were prepared. Nylon-6 nanofibers were electrospun from a solution of 20% nylon-6 in formic acid. The resulted fibers

were uniform and had diameters of 100-300 nm. Figure 7 showed a piece of gas barrier film from Li^+-fluorohectorite and nylon-6 fibers, which was about 15 cm across. The composite film was light weight with a mass per unit area of $9g/m^2$ and a thickness of 10 micrometers according to the scanning electron micrograph (Inset in Figure 7).

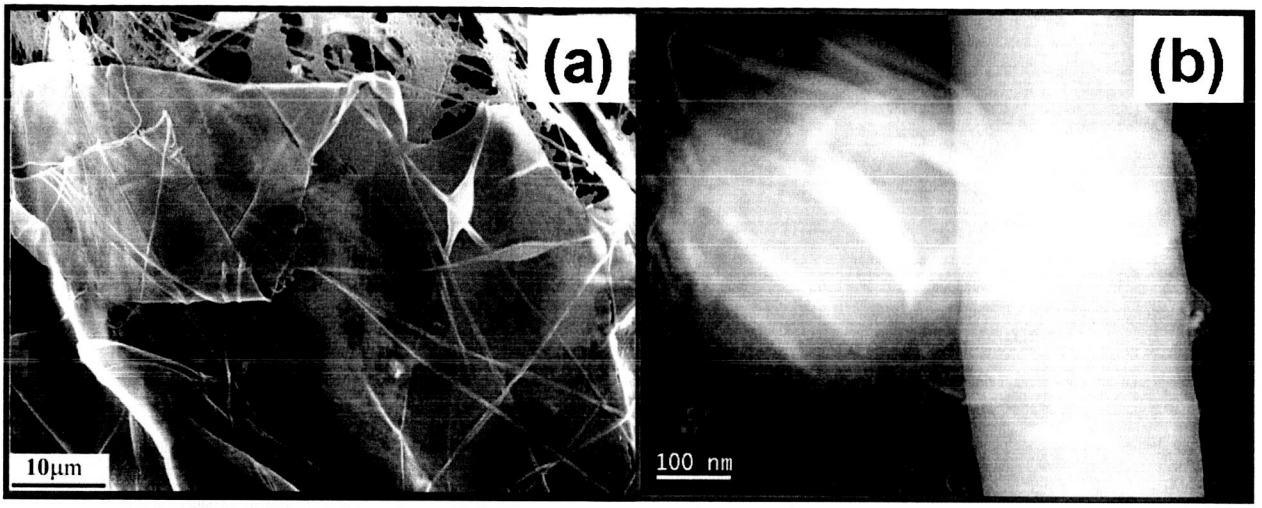

Figure 8. (a) A spincoated film of polyimide (6FDA PMFB) with clay sheets reinforced by Polyimide (BPADA BAPP) fibers; (b) Negative micrograph shows that the clay sheets tended to rest on a fiber.

Polyimide (BPADA BAPP) fibers were electrospun from a solution of polyimide in dimethylacetamide on a glass cover slide. A solution of polyimide (6FDA PMFB) containing montmorillonite in acetone was spincoated on the glass slide with electrospun fibers. The resulted film was floated on water and observed by scanning electron microscopy. Although film was ultra thin, it was strong enough to be handled with care. The film was picked up by a pair of forceps and folding was produced to show flexibility of the film. A film, about a few hundred nanometers thick, was observed in a scanning electron micrograph (Figure 8a). Nanofibers were completely buried inside the polyimide film. At higher magnifications, arrangement of clay sheets in the vicinity of electrospun fibers was explored. The clay layers tended to lie flat in the thin film when they were in contact with electrospun fibers, which indicated a partial orientation of clay sheets in the vicinity of fibers (Figure 8b). Spincoating is a process of polymer solution flowing radially outward and solvent evaporating during the flow. During the flow, clay sheets floated in the polymer solution and moved outward. Because the

thickness of the film is comparable to the diameter of fibers, clay sheets tended to rest on a fiber when they hit a fiber. The phenomenon can be visualized by imagining leaves floating along a creek rested on a log. The induced orientation may help to improve not only the gas barrier properties but also to increase the strength and stiffness of the composite film.

4. Summary

Polymer solutions, containing clay sheets, were electrospun into nanofibers and microfibers that contained clay sheets inside. Controllable removal of polymer by plasma etching from the surface of fibers revealed the arrangement of clay. The shape, flexibility, size distribution and arrangement of clay sheets were observed by transmission and scanning electron microscopy. The clay sheets were partially aligned in big fibers with normal direction of clay sheets perpendicular to fiber axis. Crumpling of clay sheets inside fibers was observed when the fiber diameter was comparable to the lateral size of clay sheets. Single sheets of clay were observed both by catching clay sheets dispersed in water with electrospun nanofiber mats and by the deliberate removal of most of the polymer in the fibers.

Thin, flexible gas barrier films, that are reasonably strong, were assembled from clay sheets and polymer nanofibers. Structure of composite films was characterized with scanning electron microscopy. Continuous film of clay sheets were physically attached to the surface of fiber mats. Spincoating film of polymer and clay sheets was reinforced by electrospun fiber scaffold. Certain alignment of clay sheets was observed in the vicinity of fibers.